

Superconductivity in graphite intercalation compounds

Robert P Smith[†], Thomas E Weller[‡], Christopher A Howard[‡], Mark P M Dean^{*}, Kaveh C Rahnejat[‡], Siddharth S Saxena[†] and Mark Ellerby[‡]

[†] *Cavendish Laboratory, University of Cambridge, Madingley Road, Cambridge CB3 0HE, UK*

[‡] *Department of Physics and Astronomy, University College of London, Gower Street, London WC1E 6BT, UK*

^{*} *Department of Condensed Matter Physics and Materials Science, Brookhaven National Laboratory, Upton, New York 11973, USA*

Abstract

The field of superconductivity in the class of materials known as graphite intercalation compounds has a history dating back to the 1960s [1,2]. This paper recontextualizes the field in light of the discovery of superconductivity in CaC₆ and YbC₆ in 2005. In what follows, we outline the crystal structure and electronic structure of these and related compounds. We go on to experiments addressing the superconducting energy gap, lattice dynamics, pressure dependence, and how this relates to theoretical studies. The bulk of the evidence strongly supports a BCS superconducting state. However, important questions remain regarding which electronic states and phonon modes are most important for superconductivity and whether current theoretical techniques can fully describe the dependence of the superconducting transition temperature on pressure and chemical composition.

Corresponding author. Tel: +44 (0)7792954220 fax: +44 (0)20 7679 7145
e-mail address: mark.ellerby@ucl.ac.uk (Mark Ellerby).

Key words: intercalation, superconductivity, graphite, low-dimension

1.1 Introduction

Within the field of superconductivity some of the most interesting outstanding issues concern the role of dimensionality and magnetism in superconducting pairing. For ex-

ample, the superconducting transition temperature of CeIn_3 increases by an order of magnitude on going from three-dimensional CeIn_3 to quasi two-dimensional CeIn_3 layers in the Ce_{15} compounds [4, 5, 6]. The perspective of quasi two-dimensional compounds in which superconductivity plays a role opens a further class of materials, the dicalcogenides, examples of which are NbSe_2 [7] and TiSe_2 [8]. Furthermore, superconductivity in two-dimensional materials is often found in close proximity to other electronic ground states such as charge density wave (CDW) states. However the underlying mechanisms that support the superconducting ground-state form an important motivation for choosing to study graphite intercalation compounds (GICs) as, perhaps contentiously, the most canonical low dimensional environment. The two main general reviews of this field are Dresselhaus and Dresselhaus [1] and Enoki, Suzuki and Endo [2].

In the examples of the materials given above, an important component under investigation is the impact of charge transfer in the emergence of novel ground-states of low dimensional systems; superconductivity being an important example. Turning now to graphite as a host for new ground-states, the question arises as to how the charge transfer from the intercalant to the graphene sheets can be adjusted. This can be readily achieved through changing the intercalant in the graphite host. As indicated in Dresselhaus and Enoki [1, 2], considerable effort has been made in this field and more recently two different but parallel discoveries have been made. The most important of these, and the one with most impact, is the discovery of the formation of a single sheet of graphene, the building block of graphite [9]. However, the present work concerns the discovery presented by Weller *et al* [10], that a large electronic charge transfer to the graphene sheets achieved by the intercalation of graphite with Ca and Yb, led to considerably higher transition temperatures (T_C 's) than earlier work. This work [10] has reinvigorated activity into superconductivity in GICs. Understanding the mechanism of superconductivity in GICs is relevant to the physics of graphene at high electron doping, [9] and has led to, as yet unconfirmed, predictions of superconductivity in metal decorated single layer graphene sheets [11].

Our search for superconductivity at elevated temperatures in GICs focused on increasing charge transfer from the intercalant to the graphene sheets. In particular, this led to the motivation for choosing to intercalate ytterbium (which has a propensity to lie on the border between nonmagnetic Yb^{2+} and magnetic Yb^{3+} ions) into the quasi two-dimensional graphite structure, perhaps suggesting the importance of magnetic interactions. However this notion was immediately dismissed when, calcium, which is a similar size to ytterbium, and forms a 2+ nonmagnetic ion, was intercalated and also found to superconduct. Importantly, Weller *et al.*'s work [10] was corroborated and improved on in the work of Emery *et al.* [12] in the case of CaC_6 , by confirming superconductivity on samples of CaC_6 of much higher quality. It is worth pointing out that the novel technique

used to prepare samples in [12] used the methods established by Pruvost *et al* in two key papers [13, 14]. The studies [10, 12] have extended the field of GICs and provide clear models with which to study the effect of both charge transfer and possible magnetic fluctuations on the quasi two-dimensional graphite system.

1.2 Background to Graphite Intercalate Superconductors

1.2.1 Structure

Graphite is composed of two-dimensional hexagonal sheets of carbon held together by weak Van der Waals forces generally in an ABAB stacking arrangement [1, 2]. In GICs layers of intercalant atoms (in all the cases mentioned here these are metals) form between these graphite sheets. The number of graphite sheets between each intercalant layer is described by the so-called staging of the GIC. So in a stage one GIC the intercalant and graphite layers are alternate whereas in a stage-2 GIC there are two graphite sheets between each intercalant layer. In general, the graphite sheets in simple stage-1 GICs form in an AAA stacking arrangement. This leaves, what are sometimes referred to as galleries, in the centre of, and in between, the hexagons of adjacent graphite layers. As each carbon atom in a hexagon is shared by three hexagons in total, if every gallery were taken then a compound of the form MC_2 would be formed. However, such compounds can only be formed by high pressure fabrication techniques and so GICs with every third or fourth gallery occupied are more common. In these cases there are several possible stacking arrangements. For example a MC_6 GIC could have a $A\alpha A\alpha A\alpha$, $A\alpha A\beta A\alpha$ or an $A\alpha A\beta A\gamma$ (here the Roman capitals stand for the graphite layers and the Greek letters for the intercalant layers) stacking structure. Having said this, as the metal ions are positive they will generally keep as far away from one another as possible and so the $A\alpha A\alpha A\alpha$ structure is unlikely, and indeed only found in LiC_6 . A further effect on the structure of intercalation is to push the graphite layers further apart.

1.2.2 Electronic structure

The electronic structure of GICs can be understood by considering the bonding within the graphite layers. Carbon has an outer electronic structure $2s^2 2p^2$ and in graphite three of these outer electrons go into forming three sp^2 (σ bonds) like orbitals and hence an hexagonal graphite layer is formed. This leaves one electron per carbon in the p_z orbital. These p_z orbitals hybridise with one another to form the π and π^* bands [1, 2]. In a single layer the gap between the π and π^* bands is zero in two directions in k -space leading to a

point like Fermi surface and hence a zero band gap semiconductor having linear ‘Dirac-like’ dispersion which can lead to many interesting properties [9]. On increasing the number of layers the π and π^* bands overlap slightly in certain k -space directions. This results in a π band with a small number of holes and a π^* band with a small number of electrons. In fact the number of holes and electrons are very similar and this leads to some interesting properties such as a large magnetoresistance [15, 16].

Graphite Intercalate	T_c / K	Stage	M_{c2}^2/M_{c2}^1	No of intercalant atoms per C
LiC ₆	–	1	na	1/6
LiC ₃	–	1	na	1/3
LiC ₂	1.9	1	na	1/2
NaC ₆	–	1	na	1/6
NaC ₄	2.8	1	na	1/4
NaC ₃	3.5	1	na	1/3
NaC ₂	5	1	na	1/2
KC ₂₄	–	2	–	1/24
KC ₈	0.15	1	4-6	1/8
KC ₆	1.5	1	2-3	1/6
KC ₃	3	1	1.1	1/3
RbC ₈	0.02	1	2-3	1/8
CsC ₈	–	1	–	1/8

Table 1: The transition temperatures of elemental graphite intercalate systems. Data taken from [17, 18, 19, 20, 21, 22 ,23].

The effect of intercalating a metallic element on the electronic band structure of the intercalated material is in general two-fold. Firstly, the metal donates some electrons to the graphite π^* band. The Fermi-surface starts out as small pockets and if there are enough electrons a full cylindrical Fermi-surface is formed and the Dirac point is moved to below the Fermi level. Secondly (assuming the intercalant is an s-metal), if not all s-electrons are donated to the graphite then there will also be an s-like intercalant derived electronic band.

1.2.3 Superconductivity

Since the discovery of the first graphite intercalate superconductor, KC₈ [18, 23], many other GICs have been made and found to be superconducting. Tables 1 and 2 provide lists

of some GICs alongside their transition temperatures. A dash indicates that the compound is not superconducting down to the lowest temperature measured.

Since the discovery of superconductivity in GICs there has been considerable debate about the mechanism and the electrons responsible for the superconductivity. The question has centered on whether the electrons responsible

Graphite Intercalate	T_c / K	Stage	Intercalant T_c	$H_{c2}^{\perp}/H_{c2}^{\parallel}$
KHgC ₄	0.73	1	0.94	10-12
KHgC ₈	1.9	2	0.94	15-30
RbHgC ₄	0.99	1	1.17	20-40
RbHgC ₈	1.40	2	1.17	10
KTl _{1.5} C ₄	2.7	1	Tl - 2.38	5
KTl _{1.5} C ₈	2.45	2	Tl - 2.38	5

Table 2: The transition temperatures of graphite intercalate systems with binary intercalates. In all of these the intercalant compound or one of the intercalant elements is superconducting. Data taken from [17, 24, 25].

for the superconductivity reside in the graphite π^* -bands, the intercalant bands or a combination of both. The relevant experimental results that must be explained are the trend in T_c between the different GICs and the anisotropy of the superconducting upper critical field (see table 2).

If the intercalant completely ionizes and its role is just to exclusively donate electrons to graphite π -bands then one would expect a trend in the transition temperatures of the GICs related to the number of electrons per carbon that the intercalant donates. It is readily apparent this assumption does not explain the superconductivity: KC₈, in which there is nominally 1/8 e per carbon donated, superconducts while LiC₆, in which there is nominally 1/6 e per carbon donated does not superconduct. On the other hand there is such a trend within particular GIC families such as the Na-C and Li-C systems (see table 1). The opposite trend is seen in the KHg-C and RbHg-C systems. Overall these facts suggest that the role of the intercalant is more complicated than that of just an electron donor or that the charge is not always simply donated to the π^* -bands.

The second key question to examine concerns the anisotropy of the superconductivity. The anisotropy of H_{c2} is defined by $H_{c2}^{\perp}/H_{c2}^{\parallel}$, where \parallel and \perp refer to the field applied parallel and perpendicular to the c -axis respectively. This anisotropy is as large as 40 in some systems [17] and has been explained within an effective mass model [17, 18] in which the anisotropy in H_{c2} is due to anisotropy in the effective mass. The critical field is related

to the coherence length in a plane perpendicular to the field, therefore

$$H_{c2}^{\parallel} = \frac{\Phi_0}{2\pi\xi_{ab}^2} \quad (1.1)$$

$$H_{c2}^{\perp} = \frac{\Phi_0}{2\pi\xi_{ab}\xi_c} \quad (1.2)$$

In the effective mass model the anisotropy in ξ is solely due to the anisotropy in the effective mass such that $\xi_{ab}/\xi_c = (m_c/m_{ab})^{1/2}$, therefore

$$\frac{H_{c2}^{\perp}}{H_{c2}^{\parallel}} = \left(\frac{m_c}{m_{ab}} \right)^{1/2} \quad 1.3$$

This model can be extended to give the angular dependence of H_{c2} and seems to work well. This suggests a large anisotropy in the effective mass of the superconducting electrons which would point towards an important role for the graphite π^* -bands as these are thought to be more anisotropic than the intercalant bands.

Thus, it appears that the superconductivity cannot be explained by either assuming the relevant electrons are exclusively in the graphite π^* band or the intercalant s -band. Historically, this reasoning led to a proposed two band model [21, 26, 27] for the superconductivity in which both bands are crucial for superconductivity. While this model is required to explain several important trends, until recently further details have been lacking.

1.3 Reframing of Superconductivity in Graphite Intercalates

As indicated in [1, 2] the preparation of GICs usually uses a technique known as vapour transport. In the case of YbC_6 , this technique works well in the sense that large areas of pure phase regions of this material form, it is also clear that, depending on the nature of the starting graphite, the intercalation is not always achieved throughout the sample, as demonstrated by the scanning electron micrograph of YbC_6 shown figure 1.1. However, complete intercalation of YbC_6 , SrC_6 and BaC_6 has been shown to be possible via vapour transport on single crystal flakes [50,28]

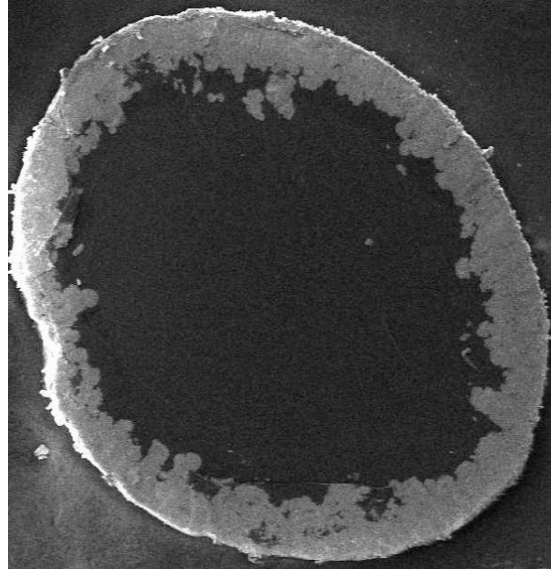


Figure 1.1: Scanning electron microscope image of a sample of YbC₆ used for the resistivity measurements in reference [10]. The white region round the edge is intercalated YbC₆ and the dark region in the centre is un-intercalated graphite. This sample is approximately XXXXX mm across.

However, in some cases, such as CaC₆ vapour transport yields limited intercalation [10, 29] and so liquid alloy flux techniques are employed, for example in CaC₆, using lithium as a transport flux. This is the technique developed by Pruvost *et al* [13, 14] and used to prepare a number of the intercalation compounds such as CaC₆, and BaC₆. However, this method leads to only a small yield of SrC₆ and has not been successful in forming MgC₆. In addition it is important to be clear of the crystal structures. For example while our two examples, YbC₆ and CaC₆, have similar structural motifs, their detailed crystal structures differ: P6₃/mmc (AαAβAα stacking) for YbC₆ and R-3m (AαAβAγ stacking) for CaC₆. These two structures are presented in figure 1.2.

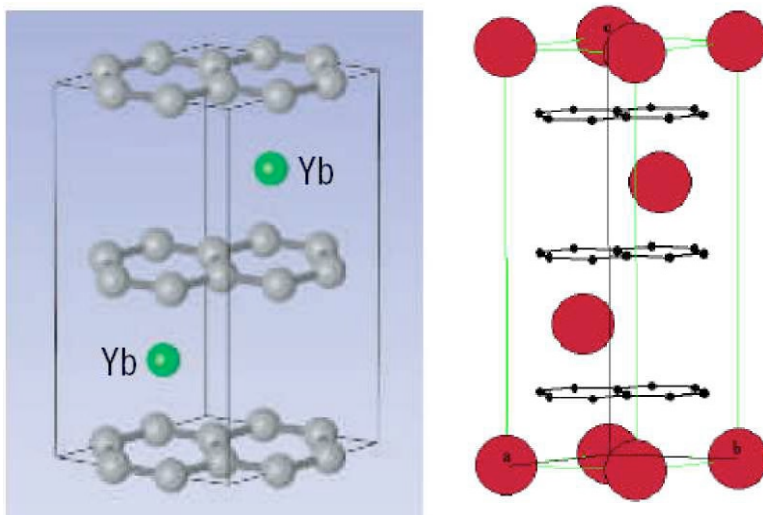


Figure 1.2: The crystal structure of YbC_6 (left) and CaC_6 (right). YbC_6 has $A\alpha A\beta A\alpha$ stacking and CaC_6 $A\alpha A\beta A\gamma$ stacking.

In fact for MC_6 GICs, CaC_6 and LiC_6 are the only two compounds that do not form a $P6_3/mmc$ structure, the latter having a $P6/mmm$ ($A\alpha A\alpha A\alpha$) structure [30-32].

1.3.1 Superconducting Phase diagrams

While considerable work has been carried out on superconductivity in the GICs, the first area of importance for the newer members of this class was the establishment of the magnetic and pressure phase diagrams, using resistivity and magnetization measurements. For YbC_6 [10] and CaC_6 [12] these phase diagrams are presented in figure 3. It is clear from these figures, that this class of compounds are type-II superconductors. From the study of H_{c2} , it has been possible to determine the superconducting coherence length both perpendicular and parallel to the c -axis. The results of these are presented in table 3.

Graphite Intercalate	T_c / K	ξ_{ab} (nm)	ξ_c (nm)	Reference
CaC_6	11.5	34	20	[10]
	11.5	35	15	[12]
	11.4	36	13	[30]
YbC_6	6.5	45	25	[10]
SrC_6	1.65	150	70	[28]

Table 3: The transition temperatures and coherence lengths for three recently discovered graphite intercalate superconductors, CaC_6 , YbC_6 and SrC_6 , revealing trends in T_c . BaC_6 has not been found to superconduct and has hence been excluded.

As can be seen from both figure 1.3 and table 3 there is a variation in T_c . In order to search for any trends several groups have made a number of measurements to explore the impact of pressure. Figure 1.4 presents the pressure phase diagrams for both YbC_6 [34] and CaC_6 [35]. In addition the work on SrC_6 is presented in the inset plot in figure 1.5(b) [28]. What is clear from figure 1.4 is the nearly linear increase of T_c as a function of increasing

pressure and is consistent with figure 1.5b (inset). Furthermore, by comparing T_c across a range of GICs figure 1.5b demonstrates that the trend of T_c with pressure can, in fact, be simplified to a trend in T_c with graphene layer separation: for the superconducting stage 1 GICs, the smaller the layer separation the larger T_c . However, this increase is at odds with the work on KHgC_4 and KHgC_8 [17] which have a decrease of T_c with increasing pressure and reveal hysteresis under pressure suggested [17] to be due to a structural transition. Moreover, in figure 1.4 shows that for YbC_6 and CaC_6 at high pressures there is eventually a decrease in T_c although the nature of this decrease differs for each system.

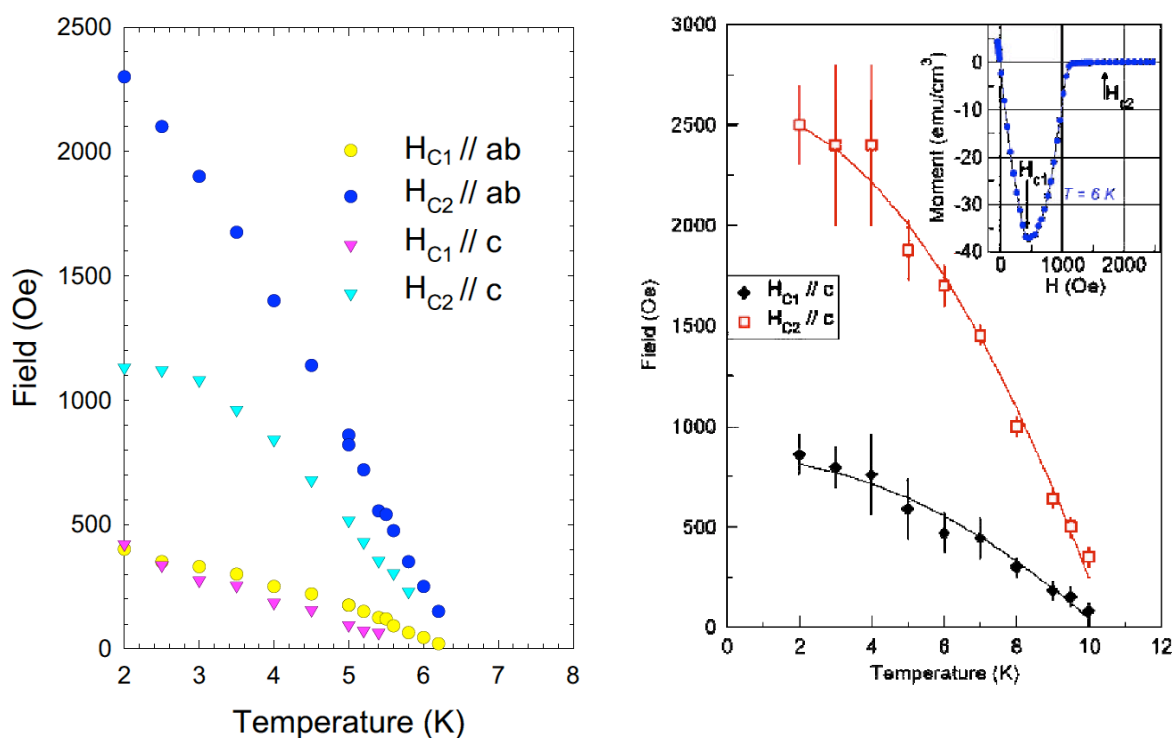


Figure 1.3: (left) magnetic phase diagram of YbC_6 for both basal plane and c -axis taken from [10]. (right) Magnetic phase diagram of CaC_6 for the c -axis taken from [12]. Both diagrams are a summary of magnetization studies.

This difference is the point at which the transition temperature begins to decrease. For YbC_6 this occurs at approximately 2 GPa whilst in CaC_6 this occurs at approximately 8 GPa. In the case of CaC_6 there was a suggestion [35] that the decrease can be attributed to a structural transition and a subsequent paper confirmed an order to disorder transition at this pressure with no apparent change in space group [36]. This onset of disorder is consistent with the interpretation of the increase in residual resistivity reported in [35]. In addition, there is a degree of structural hysteresis on decrease of the pressure reported in [36]. In the case of YbC_6 there is no published data concerning higher pressure work. However, in a private communication [37] there is X-ray high pressure data which shows a structural transition in

YbC_6 at approximately 5 GPa whilst there is no apparent transition at 2 GPa. This may suggest that in the case of YbC_6 there may be some other transition that leads to the downturn in the superconducting transition. One interesting possibility would be the emergence of a magnetic Yb^{3+} state at high pressures.

Figure 1.5 presents an overall phase diagram summary of the superconducting state in the GICs. There are two approaches to this summary, charge transfer and crystal structure.

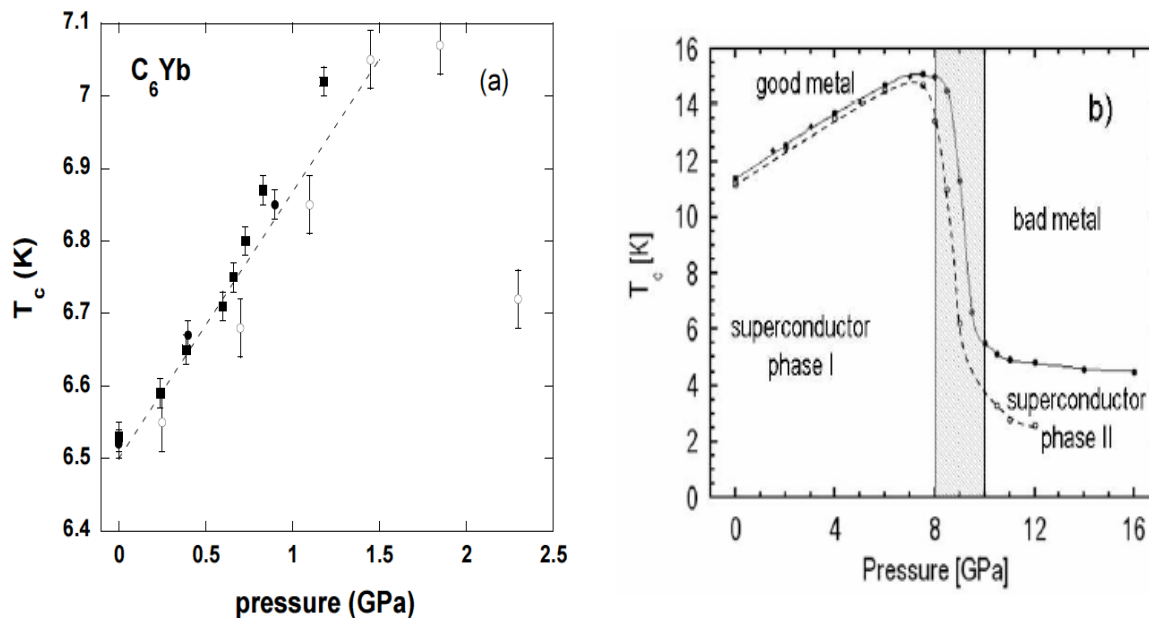


Figure 1.4 The pressure dependence of superconducting transition, T_c , of YbC_6 and CaC_6 . (a) is YbC_6 points marked by (■) corresponds to magnetization data whilst resistivity is represented by (●) and (○)[34]. (b) is CaC_6 with the dashed line (guide to eye) representing the onset transition temperature and the solid line completion of transition [35].

Considering first the charge transfer in figure 1.5(a), it is clear that for the earlier alkali intercalates (not including YbC_6 and CaC_6), including the ternary systems, there is a broad dome. Out of this there appears a second line which rises to CaC_6 . However this figure assumes a fixed charge transfer and does not incorporate the effects of pressure. The trend in T_c with layer separation shown in Fig. 5(b) is far more compelling.

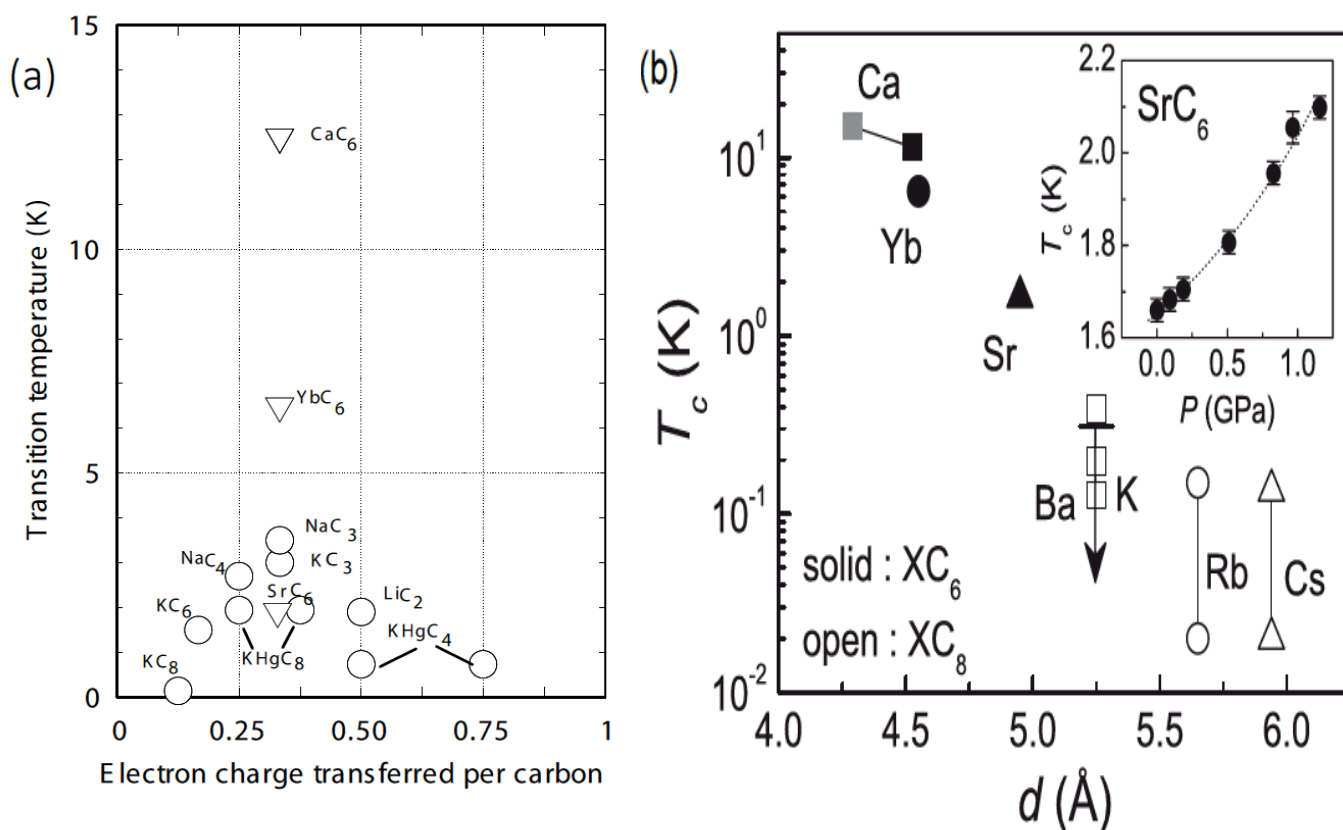


Figure 1.5 (a) Summary of superconducting transition temperatures for known [1, 2] graphite intercalation compounds with (○) the inclusion of the alkali earth compounds (▽). The ternary compounds, KHgC_8 and KHgC_4 , appear twice due to the ambiguity in the charge state of the mercury. (b) taken from [28] T_c as a function of the graphite layer separation distance, d for the alkali GICs, XC_8 ($X = \text{K}, \text{Rb}, \text{and Cs}$), and the alkaline-earth GICs XC_6 ($X = \text{Ca}, \text{Yb}, \text{Sr}, \text{and Ba}$). For CaC_6 , T_c at high pressure ($P = 8$ GPa) [32] is also plotted (gray square), and the graphite layer distance for the compressed CaC_6 is estimated from the theoretically calculated bulk modulus. The upper limit of T_c for BaC_6 is indicated by the arrow. The inset shows T_c vs pressure for SrC_6 .

1.3.2 Empirical aspects of the superconducting ground-state in GICs

Section 1.3.1 provides an outline mapping of this field which raised some questions, reawakened by the addition of three new members of this class of materials, concerning the nature of the superconducting ground-state in the GICs.

One of these questions was what is the nature of the superconducting order parameter? In other words is the superconducting gap isotropic across the Fermi-surface (*s*-wave) and if not what is the symmetry of the gap (*p*-wave, *d*-wave etc). In addition, when considering the mechanism and the electrons responsible for the superconductivity it is useful to ascertain if there is a single superconducting gap energy or several different

superconducting energy gaps as suggested by Al Jishi *et al* [38].

Magnetic penetration depth measurements on CaC_6 [39] suggest an *s*-wave pairing with a single uniform energy gap of $\Delta(0) = (1.79 \pm 0.08)$ meV. These measurements are supported by Scanning Tunneling Spectroscopy [40] which shows that CaC_6 has a single isotropic gap of 1.6 ± 0.2 meV. In addition, heat capacity measurements by Kim *et al* [33] also confirm a fully gapped superconductor and the authors suggest that their data is consistent with an electron phonon coupling of $\lambda = 0.70 \pm 0.04$. In addition, the thermal conductivity measurements on YbC_6 [41] also point to *s*-wave pairing with a single uniform energy gap. Later work of Gonnelli *et al* [42] using point contact spectroscopy have refined this view pointing out that there is some evidence for anisotropy such that $\Delta_{ab}(0) = (1.35 \pm 0.19)$ meV and $\Delta_c(0) = (1.70 \pm 0.35)$ meV so that the consistent view is of a single, possibly anisotropic, gap forming the superconducting state. It therefore quickly established that the pairing was *s*-wave with a BCS mechanism responsible for superconductivity. In fact this was also proposed shortly after Weller *et al*'s discovery, as a result of a density functional theory (DFT) study of CaC_6 [45]. This model proposed that both π^* and intercalant based bands were involved with superconductivity coupling predominantly via low energy in-plane intercalant, and higher energy out-of-plane carbon phonons. The experimental focus then shifted to confirm the identities of the phonons and electrons involved.

This was first examined via the isotope effect. In the BCS model of superconductivity this is generally characterised by α which is defined by $T_c \propto M^{-\alpha}$, where M is the atomic mass. In the weak coupling version of BCS theory for elements, alpha is given by 0.5. In some elemental superconductors α is reduced due to strong coupling effects and in compounds the isotope effect on any particular element in the compound will depend on the particular phonon modes responsible for the pairing.

Following initial suggestions of Mazin *et al* [44] that the difference in T_c between CaC_6 and

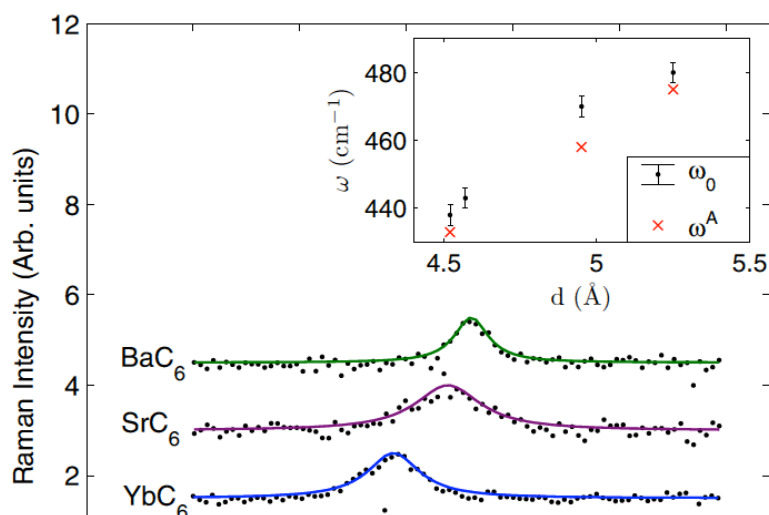


Figure 1.6 The Raman spectra of the C_z modes for XC_6 ($X = \text{Ca}, \text{Yb}, \text{Sr}, \text{Ba}$). Black dots represent the data points and the solid lines are the Lorentzian fits. The inset shows the variation in peak position for the experimental frequency ω_0 (dots) and the layer spacing d , alongside adiabatic DFT calculated values ω^A .

YbC₆ could be related to a BCS pseudo-isotope effect, Hinks et al. [40] measured the Ca isotope effect in CaC₆. Hinks measured a large isotope effect with $\alpha = 0.50 \pm 0.07$ for Ca, suggesting that the superconductivity is due mainly to calcium phonon modes. It should be mentioned experimental measurements of the phonons in these materials revealed no measurable anomalies or significant deviation from the DFT predictions [46-49]. Trends with the mass of the intercalant atoms were also observed in a Raman study [50] of XC₆ (X = Ca, Yb, Sr, Ba), figure 1.6, showing that there is a softening of the out of plane, C_z, graphene based phonons, which also agreed with theoretical predictions of the energy of modes. However, the same work revealed strong electron-phonon coupling existed with C_{xy} phonons, which did not agree with the adiabatic DFT calculations for this mode (near to the Gamma point where Raman spectroscopy probes at least). If these in-plane phonons were indeed responsible for superconductivity, they could only couple to the 2D π^* bands. This view was, in fact, proposed following the first detailed electronic structure measurements of CaC₆, with angle resolved photoemission spectroscopy (ARPES) and strengthened following further measurements of LiC₆ and KC₈ by the same authors [51,52]. ARPES permits an extraction of the magnitude of the electron-phonon coupling via analysis of the kinks in the band structure as the electrons are renormalized via their interaction with phonons. The authors showed that given the size of electron-phonon coupling, which occurred at energies equivalent to C_{xy} phonons, could explain T_c without the need of further contributions. In contrast, Sugawara et al. found no superconducting gap on the π^* band but reported a feature at the CaC₆ Gamma point which did develop a superconducting gap which that the authors attributed to an interlayer (IL) band derived from the intercalant [53]. It was only very recently that another thorough APRES study on very high quality single crystal samples unambiguously uncovered that not only the IL band but the folded π^* bands exist in close proximity near Gamma [54]. Furthermore, this work measured superconducting gaps on both π^* and IL bands. Moreover, an analysis of the relative coupling strengths revealed that, crucial to the superconductivity occurring was an interaction *between* these two bands, which can couple via C_z (out of plane) phonons. This study most closely confirms the theoretical picture proposed by Calandra and Mauri [45].

The introduction referred to the potential for charge transfer in YbC₆ resulting from intermediate valance states observed in a number of ytterbium compounds and this is referred to in figure 1.5(a) based on charge transfer. One such probe of electronic states is scanning tunneling microscopy (STM). This technique allows both structural and electronic studies of materials. Scanning Tunneling spectroscopy (SPS) was first explored for CaC₆ [40] and provided a verification of the superconducting energy gap consistent with that obtained by [39, 42]. However, the work [40] was unable to obtain atomic-

resolution images of the sample. Both atomic resolution of CaC_6 and atomically resolved spectroscopy was reported in [55] for samples at $T = 78$ K. This work was of new significance since it proved for the first time the existence of the ground-state so-called charge density wave (CDW) in a GIC (figure 1.7a). This was confirmed by measuring an energy gap $\Delta \sim 240$ meV (figure 1.7b) which could be directly associated to the real space stripe periodicity. This gap is considerably larger than that of the superconducting ground-state. During the work of [55] there was a reawakening of the important early work [56] on RbC_8 and CsC_8 . Both compounds demonstrate the structural manifestation of a CDW ground-state, but were unable to rule out other effects such as intercalant surface reconstruction.

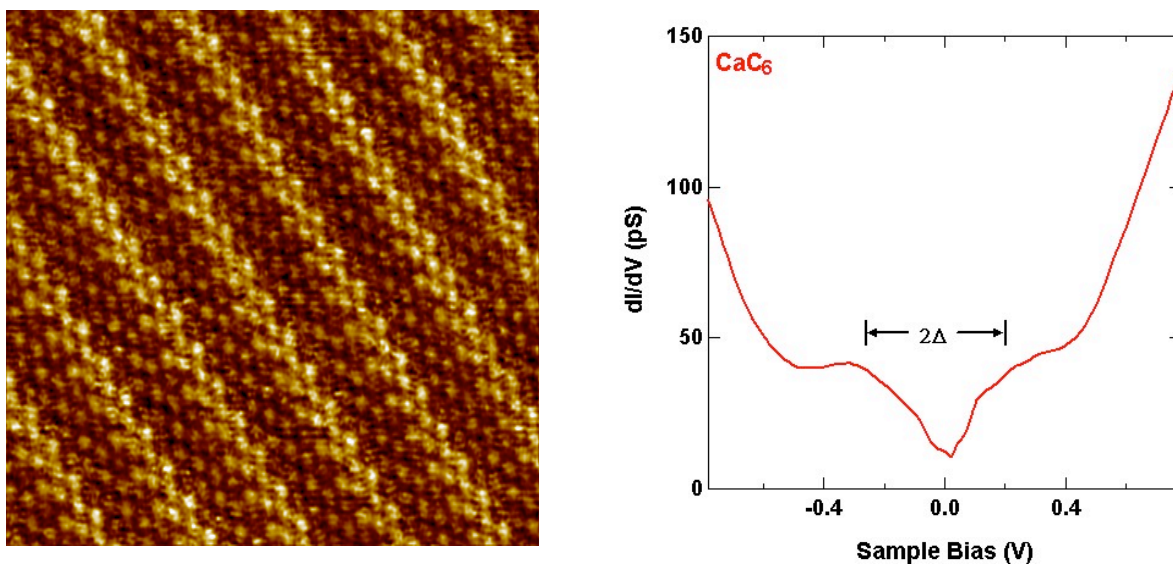


Figure 1.7: (a) The CDW structure revealed for CaC_6 at $T = 78$ K. (b) The energy gap that emerged in the CDW state with $2\Delta = 475$ meV. (Both figures taken from [45]).

1.3.3 Theoretical studies of superconductivity in GICs

The addition of the alkali-earths to this class of superconducting compounds motivated several band-structure studies, which we outline below.

Csanyi *et al* [57] claim that a pair of so-called interlayer bands are crucial to superconductivity in the GICs. These bands had been mentioned previously in regard to pure graphite [58] where they lie well above the Fermi energy. However, the addition of a metallic intercalant brings these two interlayer bands closer to the Fermi level due to both the addition of extra electrons into the graphite bands and also the increased spacing

between the layers. These calculations show that this pair of interlayer bands cross the Fermi surface in YbC_6 and CaC_6 and comparison with other intercalates, such as LiC_6 (which is not superconducting) shows that the occupation of this inter-layer band is coincident with the appearance of superconductivity (see figure 1.8). Therefore, the main conclusion of this paper [57] is that the occupation of the interlayer band is crucial for superconductivity. While accepting the occupancy of this interlayer band Calandra and Mauri [45] show that this band is in fact predominantly derived from intercalant rather than the graphite bands.

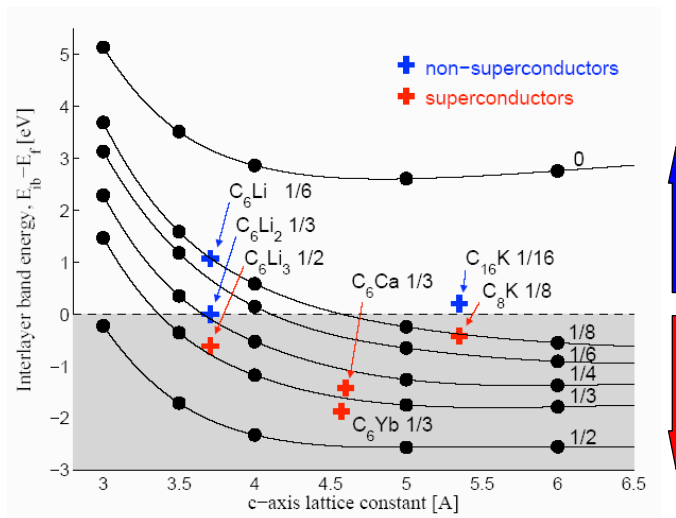


Figure 1.8 A plot of the interlayer band energy against the c -axis lattice constant showing how the occupancy of the interlayer state is concurrent with superconductivity (taken from [57]). The two main factors which effect the position of this interlayer band are c -axis spacing and electron doping. Note in particular that increasing the c -axis spacing depopulates this band.

All the band structure calculations carried out on YbC_6 show that, at ambient pressure, the $\text{Yb } f$ -bands are fully occupied and well below the Fermi level suggesting that magnetism plays no part in this system. However as pressure is applied to the system the f -electrons may move closer to the Fermi level and play an important role in the system. Calandra and Mauri extended their DFT study to include SrC_6 and BaC_6 [60]. In this work a prediction was made of the superconducting transition temperatures of $T_c=3$ K and 0.2K for SrC_6 and BaC_6 respectively. Following this prediction, as detailed earlier [28] the T_c for SrC_6 was found to be 1.65 K. In the case of BaC_6 no transition was observed, indeed in [61] no superconducting transition was found down to 80 mK.

However, the CDW state, seen in figure 1.7, was not predicted by any DFT studies. This ground-state is often driven by Jahn-Teller transitions supported by a d -state in the band structure. This d -state may exist in the two transition metal dichalcogenide compounds given as examples in the introduction. However, the d -state is less defined in the case of

CaC₆ and YbC₆. An early band structure calculations [62] on BaC₆ suggests a hybrid state of mixed *s-d* states which is close to the Fermi surface.

1.4 Summary

The pairing mechanism for superconductivity in the GICs was historically an open question given no obvious strong coupling between the electrons and phonons. Therefore, the relatively high transition temperatures in YbC₆ and CaC₆ provided a further challenge. Initially, the importance of the interlayer band points towards the answer [57]. A view which supported the framework first proposed by Calandra and Mauri [45]. These first principle calculations seem to point to a roughly equal contribution from both the intercalant and graphite phonon modes. This remains inconsistent with the reported calcium isotope effect [43]. Furthermore the large electron-phonon coupling between π^* electrons and C_{xy} phonons measured in ARPES [51,52], is in contrast with DFT predictions despite being consistent with linewidths measured in Raman Spectroscopy [50, 65], an effect also shown to evolve in graphene with increasing doping [66]. However despite these interesting discrepancies more recent ARPES reconcile the picture arising from DFT [54,45].

The increase of T_c with pressure observed in YbC₆, CaC₆ and SrC₆ has also been explained within this picture [64, 60] – as the layers decrease the overlap between π^* and IL increases, however, the rate of increase is not in full agreement. Whether the electron-phonon mechanism alone can explain the broad distribution of T_c 's observed across the range of GICs, as well as the staging dependence, is yet to be answered.

An additional mechanism for superconductivity in the GICs has been suggested [57] in which the interlayer state may provide an environment in which soft charge fluctuations promote *s-wave* superconductivity. Such a mechanism could apparently work in conjunction with phonons. It has been suggested [64] that such a mechanism is not compatible with the initial positive dependence of T_c on pressure but this is not necessarily the case [34].

There are several areas that remain unanswered. The first of these concerns the importance of MgC₆. The work of Pruvost *et al* [13, 14] may provide an indication as to how such a compound may be fabricated. However, DFT suggests that this material is unstable to formation [60]. The formation of the CDW ground-state in CaC₆ [55] is an important development. What remains to be determined is whether this ground-state is coexistent with superconductivity similar to dichalcogenides, as in the case of NbSe₂[7]. Or perhaps the CDW state is competitive with the formation of the superconducting state, similar to TiSe₂[8]. The observation of CDW, states similar to those in CaC₆, RbC₈ and CsC₈ [56], may point to the formation of a similar state in BaC₆. This has yet to be

explored.

Another question concerns the DFT prediction [60] of the superconductivity in BaC_6 since no ground-state has yet been found.

Finally, as indicated at the beginning, this reawakening of interest in superconducting GICs occurred at the same time as the discovery of the graphene sheets [9]. There is clearly activity [11] searching for a superconducting ground-state in a dressed graphene sheet material, and the work on GICs will act to inform both experimental and theoretical work on the graphene states.

Acknowledgement

We would like to acknowledge the EPSRC, the Royal Society, University College London and Cavendish Laboratory-Cambridge for their support and financial contributions. The work at Brookhaven National Laboratory was supported by the U.S. Department of Energy (DOE), Division of Materials Science, under Contract No. DE-SC0012704.

Bibliography

1. M.S. Dresselhaus, G. Dresselhaus, Intercalation compounds of graphite, *Advances in Physics*, 30, 139 1981 (reissued: 51, 1, 2002)
2. T. Enoki, M. Suzuki, and M. Endo, Graphite Intercalation Compounds and Applications, *Oxford University Press* 2003
3. N. D. Mathur, F. M. Grosche, S. R. Julian, I. R. Walker, D. M. Freye, R. K. W. Haselwimmer, and G. G. Lonzarich. Magnetically mediated superconductivity in heavy fermion compounds. *Nature*, 394:39–43, 1998
4. C. Petrovic, P. G. Pagliuso, M. F. Hundley, R. Movshovich, J. L. Sarrao, J. D. Thompson, Z. Fisk, and P. Monthoux, Superconductivity in Heavy-fermion superconductivity in CeCoIn_5 at 2.3K. *J. Phys. Condens. Matter*, 13:L337–L342, 2001.
5. J. D. Thompson, R. Movshovich, Z. Fisk, F. Bouquetc, N. J. Curroa, R. A. Fisher, P. C. Hammel, H. Hegger, M. F. Hundley, M. Jaime, P. G. Pagliuso, C. Petrovic, N. E. Phillips, and J. L. Sarrao, Superconductivity and magnetism in a new class of heavy-fermion materials. *J. Magn. Mater.*, 226-230:5–10, 2001.
6. H. Hegger, C. Petrovic, E. G. Moshopoulou, M. F. Hundley, J. L. Sarrao, Z. Fisk, and J. D. Thompson, Pressure-Induced Superconductivity in Quasi-2D CeRhIn_5 . *Phys. Rev. Lett.*, 84:4986, 2000.

7. K. Iwaya, T. Hanaguri, A. Koizumi, K. Takaki, A. Maeda and K. Kitazawa, Electronic state of NbSe₂ investigated by STM/STS, *Physica B: Cond. Mat.* 329-333, 1598 200.
8. A. F. Kusmartseva, B. Sipos, H. Berger, L. Forró, and E. Tutiš, Pressure Induced Superconductivity in Pristine 1T-TiSe₂, *Phys. Rev. Lett.* 103, 236401 2009
9. K. S. Novoselov, A. K. Geim, S. V. Morozov, D. Jiang, M. I. Katsnelson, I. V. Grigorieva, S. V. Dubonos, and A. A. Firsov, Two-dimensional gas of massless Dirac fermions in graphene. *Nature*, 438:197, 2005.
10. T. E. Weller, M. Ellerby, S. S. Saxena, R. P. Smith, and N. T. Skipper, Superconductivity in the intercalated graphite compounds C₆Yb and C₆Ca. *Nature Phys*, 1, 39 2005
11. G. Profeta, M. Calandra and F. Mauri, Phonon-mediated superconductivity in graphene by lithium deposition, *Nature Phys.*, 8,131 2012
12. N. Emery C. Hérold, M. d'Astuto, V. Garcia, Ch. Bellin, J. F. Marêché, P. Lagrange, and G. Louprias, Superconductivity of Bulk CaC₆, *Phys. Rev. Lett.*, 95, 087003 2005
13. S. Pruvost, C. Hérold, A. Hérold and P. Lagrange, On the great difficulty of intercalating lithium with a second element into graphite, *Carbon*, 41, 1281-1289 2003
14. S. Pruvost, C. Hérold, A. Hérold and P. Lagrange, Co-intercalation into graphite of lithium and sodium with an alkaline earth metal, *Carbon*, 42, 1825 2004
15. Y. Kopelevich, J. H. S. Torres, R. R. da Silva, F. Mrowka, H. Kempa, and P. Esquinazi, Reentrant Metallic Behaviour of Graphite in the Quantum Limit. *Phys. Rev. Lett.*, 90:156402, 2003.
16. X. Du, S. Tsai, D. L. Maslov, and A. F. Hebard, Metal-Insulator-Like Behaviour in Semimetallic Bismuth and Graphite. *Phys. Rev. Lett*, 94:166601, 2005.
17. Y. Iye and S. Tanuma. Superconductivity of graphite intercalation compounds - stage and pressure dependence of anisotropy. *Synt. Met.*, 5:257 & 291, 1983.
18. Y. Koike, H. Suematsu, K. Higuchi, and S. Tanuma, Superconductivity in Graphite-Alkali Metal Intercalation Compounds. *Physica B+C*, 99:503, 1980.
19. I. T. Belash, O. V. Zharikov, and A. V. Palnichenko, On the superconductivity of high pressure phases in a potassium graphite intercalation compounds C₈K. *Solid State Comm.*, 63:153-155, 1987.
20. M. Kobayashi, T. Enoki, and H. Inokuchi, Superconductivity in the first stage Rubidium graphite intercalation compound C₈Rb. *Synt. Met.*, 12:341-346, 1985.
21. I. T. Belash, A. D. Bromnikov, O. V. Zharikov, and A. V. Palnichenko, Superconductivity of graphite intercalation compounds with lithium C₂Li. *Solid State Comm.*, 69:921- 923, 1987.
22. I. T. Belash, A. D. Bromnikov, O. V. Zharikov, and A. V. Palnichenko, Effect of the metal concentration on the superconducting properties of lithium, sodium and

- potassium containing graphite intercalation compounds. *Synt. Met.*, 36:283–302, 1990.
23. N. B. Hannay, T. H. Geballe, B. T. Matthias, K. Andres, P. Schmidt, and D. MacNair, Superconductivity in Graphite Compounds. *Phys. Rev. Lett.*, 14:225, 1965.
 24. Y. Iye and S. Tanuma, Superconductivity of graphite intercalation compounds with alkali-metal amalgams. *Phys. Rev. B*, 25:4483, 1982.
 25. R. A. Wachnick, L. A. Pendry, and F. L. Vogel, Superconductivity of graphite intercalated with thalium alloys. *Solid State Comm.*, 43:5–8, 1982.
 26. R. Al-Jishi, Model for superconductivity in graphite intercalation compounds. *Phys. Rev. B*, 28:112, 1983.
 27. R. A. Jishi, M. S. Dresselhaus, and A. Chaiken, Theory of the upper critical field in graphite intercalation compounds, *Phys. Rev. B*, 44:10248, 1991.
 28. J. S. Kim, L. Boeri, F. S. Razavi and R. K. Kremer, Superconductivity in Heavy Alkaline-Earth Intercalated Graphites, *Phys. Rev. Lett.*, 99:027001, 2007
 29. G. Srinivas, C. A. Howard, S.M. Bennington, N. T. Skipper, M Ellerby, Effect of Hydrogenation on Structure and Superconducting Properties of CaC_6 . *J. Mater. Chem.* **2009**, 19, 5239
 30. D. Guerard, M. Chaabouni, P. Lagrange, M. El Makrini, and A. Hérold, Insertion de métaux alcalino-terreux dans le graphite, *Carbon*, 18, 257 1980
 31. R. Hagiwara, M. Ito, and Y. Ito. Graphite intercalation compounds of lanthanide metals prepared in molten chlorides, *Carbon*, 34(12), 1591 – 1593, 1996.
 32. M. El Makrini, D. Gurard, P. Lagrange, and A. Herold. Insertion de lanthanoides dans le graphite, *Carbon*, 18(3), 203 – 209, 1980
 33. J. S. Kim, R. K. Kremer, L. Boeri, and F. S. Razavi, Specific Heat of the Ca-Intercalated Graphite Superconductor CaC_6 . *Phys. Rev. Lett.*, 96:217002, 2006
 34. R. Smith, A. Kusmartseva, Y. T. C. Ko, S. S. Saxena, A. Akrap, L. Forro, M. Laad, T. E. Weller, M. Ellerby, and N. T. Skipper, Pressure dependence of the superconducting transition temperature in C_6Yb and C_6Ca . *Phys. Rev B*, 74:024505, 2006.
 35. A. Gauzzi, S. Takashima, N. Akeshita, C. Terakura, H. Takagi, N. Emery, C. Herold, P. Lagrange, and G. Louprias, Enhancement of Superconductivity and Evidence of Structural Instability in Intercalated Graphite CaC_6 under High Pressure, *Phys. Rev. Lett.*, 98, 067002 2007
 36. A. Gauzzi, N. Bendiab, M. d’Astuto, B. Canny, M. Calandra, F. Mauri, G. Louprias, N. Emery, C. Hérold, P. Lagrange, M. Hanfland, and M. Mezouar, Maximum T_c at the verge of a simultaneous order-disorder and lattice-softening transition in superconducting CaC_6 , *Phys. Rev. B* 78, 064506 2008.
 37. C. A. Howard and M. d’Astuto, Private communication.

38. R. A. Jishi and M. S. Dresselhaus, Superconductivity in graphite intercalation compounds. *Phys. Rev. B*, 45:12465, 1992.
39. G. Lamura, M. Aurino, G. Cifariello, E. Di Gennaro, A. Andreone, N. Emery, C. Herold, J. F. Mareche, and P. Lagrange, Experimental evidence for s-wave superconductivity in bulk CaC₆. *Phys. Rev. Lett.*, 96:107008, 2006.
40. N. Bergeal, V. Dubost, Y. Noat, W. Sacks, D. Roditchev, N. Emery, C. Herold, J. F. Mareche, P. Lagrange, and G. Loupiau, Scanning Tunneling Spectroscopy on the novel superconductor CaC₆. *Phys. Rev. Lett.*, 97, 077003 2006
41. M. Sutherland, N. Doiron-Leyraud, L. Taillefer, T. Weller, M. Ellerby, and S. S. Saxena, Bulk evidence for single-gap s-wave superconductivity in the intercalated graphite superconductor C₆Ca. *Phys. Rev. Lett.*, 98, 067003 2007
42. R. S. Gonnelli, D. Daghero, D. Delaude, M. Tortello, G. A. Ummarino, V. A. Stepanov, J. S. Kim, R. K. Kremer, A. Sanna, G. Profeta, and S. Massidda, Evidence for Gap Anisotropy in CaC₆ from Directional Point-Contact Spectroscopy, *Phys. Rev. Lett.*, 100, 207004 2008
43. D. G. Hinks, D. Rosenmann, H. Claus, M. S. Bailey, and J. D. Jorgensen, Large Ca Isotope Effect in CaC₆, *Phys. Rev. B*, 75, 014509 2007
44. I. I. Mazin, Intercalant-Driven Superconductivity in YbC₆ and CaC₆. *Phys. Rev. Lett.*, 95:227001, 2005.
45. M. Calandra and F. Mauri, Theoretical Explanation of Superconductivity in C₆Ca. *Phys. Rev. Lett.*, 95:237002, 2005.
46. A. C. Walters, C. A. Howard, M. H. Upton, M. P. M. Dean, A. Alatas, B. M. Leu, M. Ellerby, D. F. McMorrow, J. P. Hill, M. Calandra, and F. Mauri. Comparative study of the phonons in nonsuperconducting BaC₆ and superconducting CaC₆ using inelastic x-ray scattering, *Phys. Rev. B*, 84, 014511, 2011.
47. M. H. Upton, T. R. Forrest, A. C. Walters, C. A. Howard, M. Ellerby, A. H. Said, and D. F. McMorrow. Phonons and superconductivity in ybc₆ and related compounds, *Phys. Rev. B*, 82, 134515, 2010.
48. M. H. Upton, A. C. Walters, C. A. Howard, K. C. Rahnejat, M. Ellerby, J. P. Hill, D. F. McMorrow, A. Alatas, Bogdan M. Leu, and Wei Ku. Phonons in superconducting CaC₆ studied via inelastic x-ray scattering. *Phys. Rev. B*, 76, 220501, 2007.
49. M. P. M. Dean, A. C. Walters, C. A. Howard, T. E. Weller, M. Calandra, F. Mauri, M. Ellerby, S. S. Saxena, A. Ivanov, and D. F. McMorrow, Neutron scattering study of the high-energy graphitic phonons in superconducting CaC₆, *Phys. Rev. B*, 82, 014533, 2010.
50. M. P. M. Dean, C. A. Howard, S. S. Saxena and M. Ellerby, Nonadiabatic phonons within the doped graphene layers of XC₆ compounds, *Phys. Rev. B*, 81, 045405 2010.
51. T. Valla, J. Camacho, Z.-H. Pan, A. V. Fedorov, A. C. Walters, C. A. Howard, and M. Ellerby. Anisotropic electron- phonon coupling and dynamical nesting on the

- graphene sheets in superconducting CaC_6 using angle-resolved photoemission spectroscopy, *Phys. Rev. Lett.*, 102, 107007, 2009.
52. Z.-H. Pan, J. Camacho, M. H. Upton, A. V. Fedorov, C. A. Howard, M. Ellerby, and T. Valla. Electronic structure of superconducting KC_8 and nonsuperconducting LiC_6 graphite intercalation compounds: Evidence for a graphene-sheet-driven superconducting state, *Phys. Rev. Lett.*, 106, 187002, 2011.
 53. K. Sugawara, T. Sato, and T. Takahashi. Fermi-surface-dependent superconducting gap in C_6Ca . *Nature Physics*, 5, 40–43, 2009.
 54. S.-L. Yang, J. A. Sobota, C. A. Howard, C. J. Pickard, M. Hashimoto, D. H. Lu, S.-K. Mo, P. S. Kirchmann and Z.-X. Shen, Superconducting graphene sheets in CaC_6 enabled by phonon-mediated interband interactions, *Nature Communications* 5, Article number: 3493, 2014
 55. K.C. Rahnejat, C.A. Howard, N.E. Shuttleworth, S.R. Schofield, K. Iwaya, C.F. Hirjibehedin, Ch. Renner, G. Aeppli and M. Ellerby, Charge density waves in the graphene sheets of the superconductor CaC_6 , *Nature Comms* 2, Art. num.: 558 2011
 56. D. Anselmetti, V. Geiser, G. Overney, R. Wiesendanger, and H.-J. Güntherodt, Local symmetry breaking in stage-1 alkali-metal–graphite intercalation compounds studied by scanning tunneling microscopy, *Phys. Rev. B* 42, 1848(R) 1990
 57. G. Csanyi, P. B. Littlewood, A. H. Nevidomskyy, C. J. Pickard, and B. D. Simons. Electronic Structure of the Superconducting Graphite Intercalates, *Nature Phys*, 1, 42 2005.
 58. M. Posternak, A. Baldereschi, A. J. Freeman, E. Wimmer, and M. Weinert, Prediction of Electronic Interlayer States in Graphite and Reinterpretation of Alkali Bands in Graphite Intercalation Compounds. *Phys. Rev. Lett*, 50:761, 1983.
 59. I. I. Mazin, L. Boeri, O. V. Dolgov, A. A. Golubov, G. B. Bachelet, M. Giantomassi, and O. K. Andersen, Unsolved problems in superconductivity of CaC_6 . *Physica C: Superconductivity*, 460, 116 2007.
 60. M. Calandra and F. Mauri, Possibility of superconductivity in graphite intercalated with alkaline earths investigated with density functional theory, *Phys. Rev B*, 74, 094507 2006
 61. S. Nakamae, A. Gauzzi, F. Ladieu, D. L'Hôte, N. Eméry, C. Hérold, J.F. Marêché, P. Lagrange and G. Loupiau, Absence of superconductivity down to 80 mK in graphite intercalated BaC_6 , *Solid State Comms*, 145, 493 2008
 62. N. A. W. Holzwarth, D. P. Divincenzo, R. C. Tatar and S. Rabi, Energy-band structure and charge distribution for BaC_6 , *Inter J. Quantum Chem.*, 23, 1223 1983.
 63. I I Mazin and S L Molodtsov, Electrons and phonons in YbC_6 : Density functional calculations and angle-resolved photoemission measurements. *Phys. Rev. B*, 72, 172504, 2005.
 64. J. S. Kim, L. Boeri, R. K. Kremer, and F. S. Razavi, Effect of Pressure on Superconducting Ca-Intercalated Graphite CaC_6 . *Phys. Rev. B*, 74, 214513 2006

65. J. C. Chacon-Torres, L. Wirtz, and T. Pichler. Raman spectroscopy of graphite intercalation compounds: Charge transfer, strain, and electron-phonon coupling in graphene layers, *Physica Status Solidi (b)*, 251(12) 2014.
66. C. A. Howard, M. P. M. Dean, and F. Withers. Phonons in potassium-doped graphene: The effects of electron-phonon interactions, dimensionality, and adatom ordering, *Phys. Rev. B*, 84, 241404, 2011.